

Features of two-pion Bose-Einstein correlations based on event-by-event analysis in smoothed particle hydrodynamics

Yan-Yu Ren¹, Wei-Ning Zhang^{1,2*}, and Jian-Li Liu¹

¹*Department of Physics, Harbin Institute of Technology,
Harbin, Heilongjiang 150006, China*

²*School of Physics and Optoelectronic Technology,
Dalian University of Technology,
Dalian, Liaoning 116024, China*

(Dated: May 23, 2019)

We examine the space-time structure of the particle-emitting sources with fluctuating initial conditions in smoothed particle hydrodynamics. The two-pion correlation functions of single events for the sources exhibit event-by-event fluctuations. The large event-by-event fluctuations and wide distributions of the error-inverse-weighted fluctuations between the HBT correlation functions of single and mixed events are important features for the sources with event-by-event fluctuating initial conditions. The root-mean-square of the weighted fluctuations is a signal to detect the inhomogeneity of the systems produced in high energy heavy ion collisions.

PACS numbers: 25.75.-q, 25.75.Nq, 25.75.Gz

I. INTRODUCTION

The main physics goal of heavy ion collisions at Relativistic Heavy Ion Collider (RHIC) is the study of the extremely hot and dense matter, the quark-gluon plasma (QGP), formed in the early stage of the collisions. Hydrodynamics may provide a direct link between the early state of the matter and final observables and has been extensively used in high energy heavy ion collisions. The hydrodynamic calculations with the equation of state of the QGP agree well with the RHIC v_2 data of the elliptic flow at low transverse momentum $p_T < 2$ GeV [1, 2, 3, 4, 5], which is believed as an important evidence of the existence of a strongly coupled QGP in the early stages of the collisions [6, 7, 8, 9, 10]. However, hydrodynamic results can not explain the RHIC Hanbury-Brown-Twiss (HBT) measurements, $R_{\text{out}}/R_{\text{side}} \approx 1$ [11, 12, 13, 14]. It is the so-called HBT puzzle.

In Ref. [15] a granular source model of QGP droplets evolving hydrodynamically was put forth to explain the HBT puzzle. The suggestion was based on the observation that in the hydrodynamic calculations for the granular source the average particle emission time scales with the initial radius of the droplet, whereas the spacial size of the source is the scale of the distribution of the droplets. For a granular source with many of the small droplets distributed in a relatively large region, the HBT radius R_{out} can be close to R_{side} [15]. In Ref. [16] the authors further investigated the elliptic flow and HBT radii as a function of the particle transverse momentum for an improved granular source model of QGP droplets. They argued that although a granular structure was suggested earlier as the signature of a first-order phase transition

[15, 17, 18, 19, 20, 21, 22, 23, 24], the occurrence of granular structure may not be limited to first-order phase transition [16, 25]. In an event-by-event basis, the initial transverse distribution of energy density in nucleus-nucleus collisions have been known to be highly fluctuating [26, 27, 28]. This large spatial fluctuation together with surface tension effect may facilitate the occurrence of instability of the system during its violent expansion subsequently and the fragmentation to many granular droplets [16, 25]. So, the examination of the space-time structure in event-by-event basis is important to understand the system evolution and the HBT puzzle.

Smoothed Particle Hydrodynamics (SPH) is a suitable candidate that can be used to treat the system evolution with large fluctuating initial conditions for investigating event-by-event attributes in high energy heavy ion collisions [28, 29]. The main idea of SPH is the parametrization of the fluid in terms of discrete Lagrangian coordinates attached to small volumes (call ‘particles’) with some conserved quantities in hydrodynamics [28, 29, 30]. NEXSPHERIO is a SPH code [28, 31, 32] with event-by-event initial conditions generated by NEXUS event simulator [27]. It has been used to study a wide range of problems in high energy heavy ion collisions [28, 29, 31, 32, 33, 34, 35]. In this article we use NEXSPHERIO to simulate the evolution of the system produced in the collisions of $\sqrt{s_{NN}} = 200$ GeV Au+Au at RHIC. We will examine the space-time structure of the systems and investigate the two-pion HBT correlation functions in event-by-event basis. Our results show that the systems are inhomogeneous in space and time both for a first-order and a cross-over transitions between the QGP and hadronic phase. There are ‘lumps’ in different regions of the system. The two-pion HBT correlation functions in event-by-event basis exhibit large fluctuations, which lead to a wide distribution of the error-inverse-weighted fluctuations between the HBT

*wnzhang@dlut.edu.cn

correlation functions of single and mixed events. These large fluctuations and wide distributions are important features for the sources with event-by-event fluctuating initial conditions. The root-mean-square of the weighted fluctuations is a signal to detect the inhomogeneity of the systems produced in high energy heavy ion collisions.

II. SYSTEM EVOLUTION AND SPACE-TIME STRUCTURE

In hydrodynamics the behavior of system evolution is determined by the initial conditions and the equation of state (EOS) of the system. The system initial states of NEXSPHERIO are given by the NEXUS code, which can provide detailed space distributions of energy-momentum tensor, baryon-number, strangeness, and charge densities at a given initial time (which is taken to be $\tau_0 = 1$ fm in our calculations), in event-by-event basis [27, 28]. In our calculations we use two kinds of EOS. The first one, EOS-I, considers a first-order phase transition at $T_c = 160$ MeV between a QGP and a hadronic resonance gas as used in Refs. [31, 33]. The QGP is an ideal gas of massless quarks (u, d, s) and gluons and the hadronic gas contains the resonances with mass below 2.5 GeV/c², where volume correction is taken into account [31, 33]. Because at RHIC energy the net baryon constituent is very small and the phase transition is a smooth cross over, in the mid-rapidity region of the heavy ion collisions, a modification for the EOS with first-order phase transition in the hydrodynamical code should be considered [28, 34]. Accordingly, we introduce EOS-II which is obtained by smoothing the EOS-I in the transition region with the entropy density suggested by QCD lattice results [15, 36, 37, 38, 39]. Fig. 1 shows the relations of the thermodynamical quantities for the systems evolving with the EOS-I (grey) and the EOS-II (black), where s , ϵ , and P are entropy density, energy density, and pressure of the system. The width of the transition ΔT for the EOS-II is taken as $0.1T_c$ [38].

The coordinates used in NEXSPHERIO are $\tau = \sqrt{t^2 - z^2}$, x , y , and $\eta = (1/2) \ln[(t+z)/(t-z)]$ [28, 29, 31]. They are convenient for a system with rapid longitudinal expansion. However, in order to examine the space-time structure of the system we must work in the center-of-mass frame of the system. Figs. 2(a), (b), (c), and (d) are the pictures of the transverse distributions of energy density for one NEXSPHERIO event ($\sqrt{s_{NN}} = 200$ GeV Au+Au) with impact parameter $b = 0$ fm and evolving with EOS-I. The pictures are taken for the region $(|x, y| < 12$ fm and $|z| < 1$ fm) and at $t = 1, 5, 9$, and 13 fm/c with an exposure of $\Delta t = 0.3$ fm/c. Figs. 2(a'), (b'), (c'), and (d') are the pictures for the event with the same initial conditions but evolving with EOS-II. One can see that the systems are inhomogeneous in space and time both for the events evolving with the EOS-I and the EOS-II. There are many “lumps” in the systems. By comparing the pictures for different events we

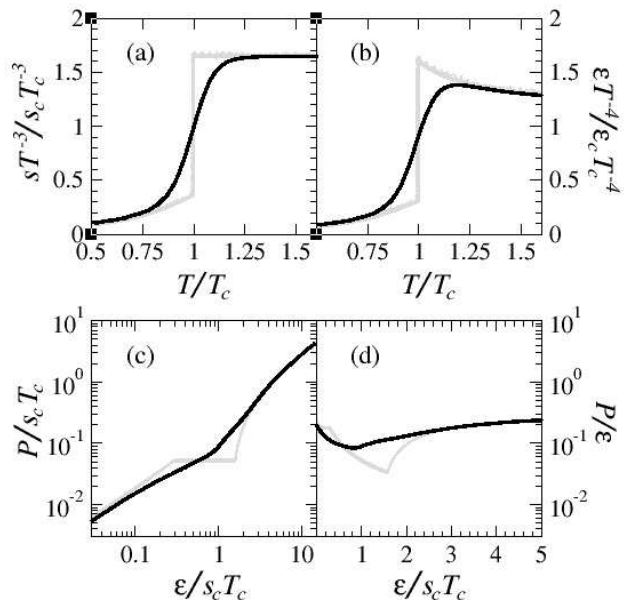


FIG. 1: (a) entropy density s , (b) energy density ϵ , (c) pressure P , and (d) P/ϵ of the systems evolving with EOS-I (grey) and EOS-II (black).

find that the lump locations are different event-by-event. Figs. 3((a)–(d)) and ((a')–(d')) show the pictures of the transverse distributions of energy density for the events with different impact parameters and evolving with EOS-I and EOS-II, respectively. One can see that the number of the lumps in the system decreases with impact parameter increasing. Because the systems evolving with the two kinds of EOSs have the similar space-time structure, we will consider only the EOS-II in our calculations later.

III. TWO-PION CORRELATION FUNCTIONS IN EVENT-BY-EVENT BASIS

Two-pion interferometry is a powerful tool for probing the space-time structure of particle-emitting source. For the source with dense and void density oscillations, the single-event HBT correlation functions will appear fluctuations relative to the mixed-event HBT correlation functions [23, 24]. The fluctuation patterns are different event-by-event.

Assuming that final identical pions are emitted at a system configuration characterized by a freeze-out temperature T_f , we may generate the pion momenta according to Bose-Einstein distribution and construct the single-event and mixed-event two-pion correlation functions [16, 24] for NEXSPHERIO events. Fig. 4 shows the two-pion correlation functions $C(q_{\text{side}}, q_{\text{out}}, q_{\text{long}})$ for the NEXSPHERIO events with different impact parameters. Here q_{side} , q_{out} , and q_{long} are the components of “side”, “out”, and “long” of relative momentum of pion pair [40, 41], which are calculated in the LCMS frame

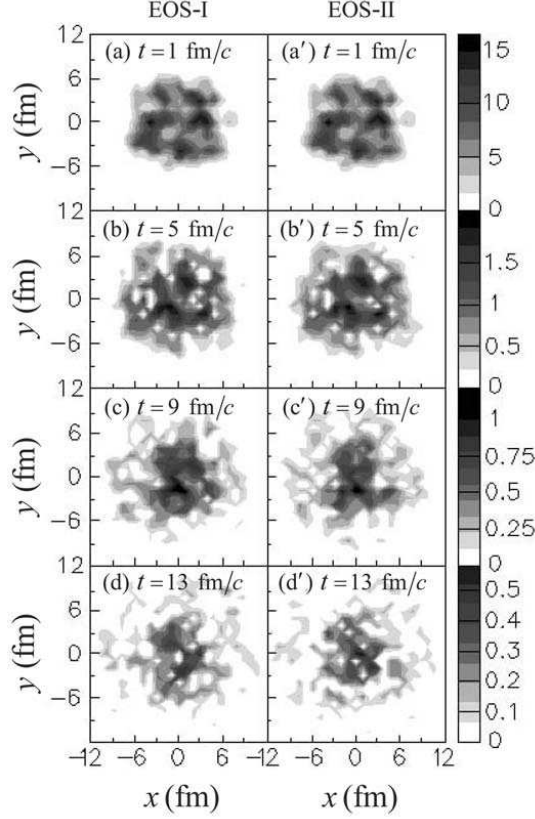


FIG. 2: Transverse distributions of energy density of the events evolving with EOS-I ((a)–(d)) and EOS-II ((a')–(d')) at different times for $\sqrt{s_{NN}} = 200$ GeV Au+Au collisions, $b = 0$ fm. The unit of energy density is GeV/fm^3 .

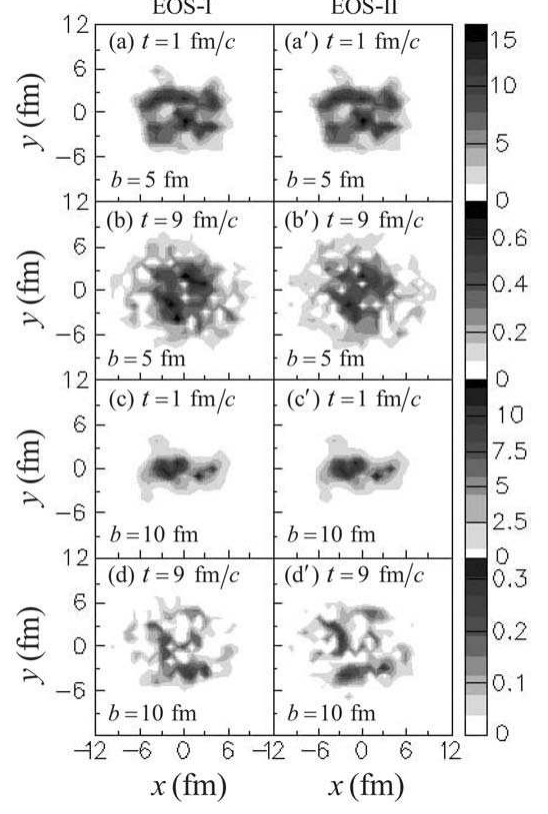


FIG. 3: Transverse distributions of energy density of the events for $\sqrt{s_{NN}} = 200$ GeV Au+Au collisions with $b = 5$ and 10 fm. The systems evolve with EOS-I ((a)–(d)) and EOS-II ((a')–(d')). The unit of energy density is GeV/fm^3 .

[12]. In each panel of Fig. 4, the dashed lines give the correlation functions for a sample of different single events and the solid line is for the mixed-event obtained by averaging over 40 single events. In the present calculations, the freeze-out temperature is taken to be 150 MeV. For each single event the total number of generated pion pairs in the relative momentum region ($q_{\text{side}}, q_{\text{out}}, q_{\text{long}} \leq 200$ MeV/c) is $N_{\pi\pi} = 10^6$ and the numbers of the pion pairs in the relative momentum regions ($q_i \leq 200$ MeV/c; $q_j, q_k \leq 30$ MeV/c) are about $2.7\%N_{\pi\pi}$, where i, j , and k denote “side”, “out”, and “long”.

From Fig. 4 it can be seen that the correlation functions for single events exhibit fluctuations relative to those for the mixed-events. These fluctuations are larger for bigger impact parameter. It is because that the number of the lumps in system decreases with the impact parameter and the fluctuations are larger for the source with smaller number of lumps [23, 24]. It also can be seen that in the longitudinal direction the correlation functions exhibit oscillations which can not be smoothed out by event mixing. This is because that there are two sub-sources moving forward and backward the beam direction. By applying an additional cut for the initial ra-

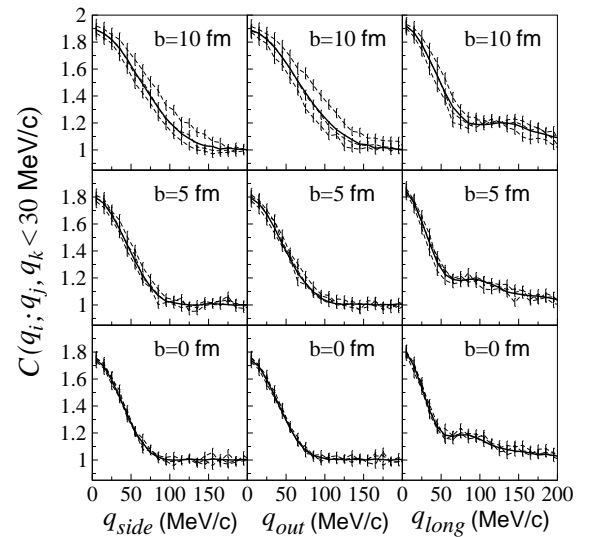


FIG. 4: Two-pion correlation functions for a sample of different single events (dashed lines) and mixed events (solid lines) for the NEXSPHERIO events with different impact parameters.

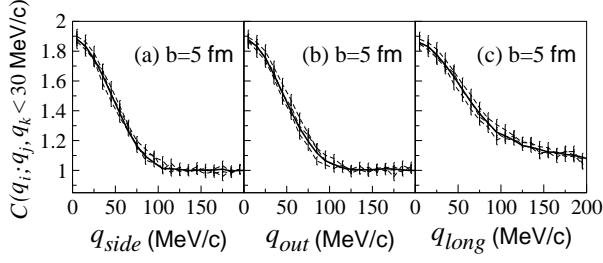


FIG. 5: Two-pion correlation functions for a sample of different single events (dashed lines) and mixed events (solid lines) with the initial rapidity cut $\eta_0 > 0$.

pidity of the “smoothed particles”, $\eta_0 > 0$, we find that the oscillations of the mixed-event correlation functions are smoothed out as shown in Fig. 5(c).

IV. DISTRIBUTION OF THE FLUCTUATION OF SINGLE-EVENT HBT CORRELATION FUNCTION

In last section we show that the two-pion correlation functions of single events exhibit event-by-event fluctuations. In realistic experimental situations, the number of identical pion pairs in each single event is limited. Traditional HBT measurements are based on mixed-event analysis because of statistics. The event-by-event fluctuations are smoothed out in the mixed-event analysis. In order to observe the event-by-event fluctuations, we next investigate the distribution dN/df of the fluctuations between the correlation functions of single and mixed events, $|C_s(q_i) - C_m(q_i)|$, with their error-inverses as weights [24],

$$f(q_i) = \frac{|C_s(q_i) - C_m(q_i)|}{\Delta|C_s(q_i) - C_m(q_i)|}. \quad (1)$$

In the calculations, we take the width of the relative momentum q_i bin as 10 MeV and use the bins in the region $20 \leq q_i \leq 200$ MeV. The up panels of Fig. 6 show the distributions of f in the “side”, “out”, and “long” directions, obtained from 40 simulated events. The impact parameter for these events is 5 fm ($b = 5$ fm) and the number of correlated pion pairs for each of these events is 10^7 ($N_{\pi\pi} = 10^7$). The thick lines are the results for the events with event-by-event fluctuating initial conditions (FIC). Because in the last analysis the fluctuations of the single-event correlation functions are from the FIC, for comparison we also investigate the distribution dN/df for the events with the smooth initial conditions (SIC) obtained by averaging over 30 random NEXUS events [28, 33, 34] (although it is not a realistic case). It can be seen that the f distributions for FIC are wider for the higher freeze-out temperature $T_f = 150$ MeV than those for the lower $T_f = 125$ MeV, and both for the freeze-out temperatures the distributions for FIC are much wider than the corresponding results for SIC. The down panels

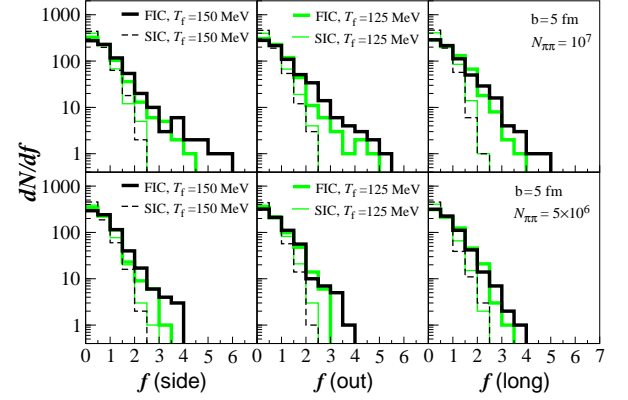


FIG. 6: The distributions dN/df for 40 events with FIC and SIC. $b = 5$ fm.

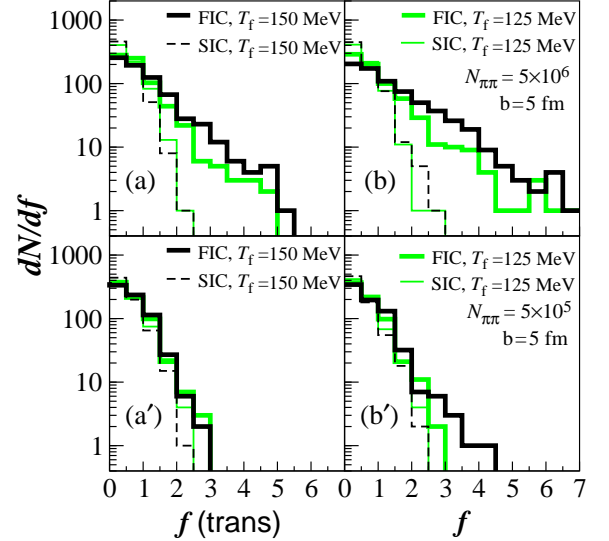


FIG. 7: The distributions dN/df for 40 events, where f are calculated for the variables of q_{trans} and q . $b = 5$ fm.

of Fig. 6 show the distributions of f for 40 simulated events with $b = 5$ fm and $N_{\pi\pi} = 5 \times 10^6$. It can be seen that the distributions for FIC are also wider than those for SIC in this case.

In experiments the number of correlated pion pairs in one event, $N_{\pi\pi}$, is limited. It is related to the energy $\sqrt{s_{NN}}$. The higher $\sqrt{s_{NN}}$ is, the larger $N_{\pi\pi}$ will be. For a finite $N_{\pi\pi}$, sometimes we have to reduce variable numbers in data analyses although it will lose some details. In Fig. 7 we show the distributions of f for the variables of the transverse relative momentum q_{trans} and the relative momentum q for 40 events with $b = 5$ fm. One can see that for $N_{\pi\pi} = 5 \times 10^6$, the distributions for FIC are much wider than those for SIC both for q_{trans} and q . Even for $N_{\pi\pi} = 5 \times 10^5$, the widths for FIC are visibly larger than those for SIC for q . In order to examine quantitatively, we calculate the root-mean-square (RMS) of the f . Fig. 8 shows the RMS f_{rms} as a function of $N_{\pi\pi}$ for the 40 events with $b = 5$ fm and $T_f = 150$ MeV. It can

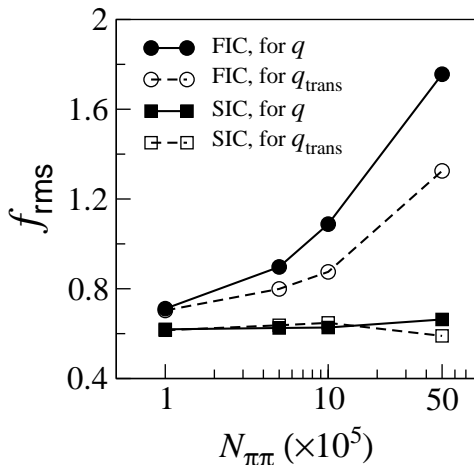


FIG. 8: The root-mean-square of f for the variables of q_{trans} and q as a function of $N_{\pi\pi}$. $b = 5$ fm and $T_f = 150$ MeV.

been seen that the values of f_{rms} rapidly increase with $N_{\pi\pi}$ for FIC because the errors in Eq. (1) are decrease with $N_{\pi\pi}$. For SIC the values of f_{rms} are almost constant. It is because that the differences in Eq. (1) also decrease with $N_{\pi\pi}$ in this case. In Figs 6, 7, and 8 we do not show the errors of the distributions and the RMS values, because they are related to the number of events and the number in experiments may be large enough.

At RHIC energy the event multiplicity of identical pions, M_π , is about several hundreds for central collisions. The order of $N_{\pi\pi}$ is about 10^5 ($M_\pi^2/2$). However, at the higher energy of Large Hadron Collider (LHC) M_π will be about two thousands and the order of $N_{\pi\pi}$ will be 10^6 . Our results show that if the particle-emitting sources at LHC energy is the inhomogeneous the RMS of f will be

much larger than that at RHIC energy. The distributions of f and their RMS are useful observables for the inhomogeneous sources.

V. CONCLUSION

In an event-by-event basis, the initial density distribution of matter in nucleus-nucleus collisions have been known to be highly fluctuating. The fluctuating initial conditions lead to event-by-event inhomogeneous particle-emitting sources. For these sources the two-pion HBT correlation functions of single events exhibit event-by-event fluctuations. Because of data statistics traditional HBT measurements are mixed-event analysis. In these measurements the fluctuations of the correlation functions of single events are smoothed out. In order to observe the fluctuations we examine the distributions of the fluctuations between the correlation functions of single and mixed events, with the weights of the error-inverses of the fluctuations. We find that the distributions and the RMS of the weighted fluctuations are useful observables for the inhomogeneous sources. If the particle-emitting sources produced in the heavy ion collisions at LHC energy are inhomogeneous, these RMS will be much larger than those at RHIC energy.

Acknowledgments

This research was supported by the National Natural Science Foundation of China under Contracts No. 10575024 and No. 10775024.

-
- [1] C. Adler *et al.* (STAR Collaboration), Phys. Rev. Lett. **87**, 182301, 2001.
 - [2] C. Adler *et al.* (STAR Collaboration), Phys. Rev. Lett. **89**, 132301, 2002.
 - [3] C. Adler *et al.* (STAR Collaboration), Phys. Rev. Lett. **90**, 032301, 2003.
 - [4] S. S. Adler *et al.* (PHENIX Collaboration), Phys. Rev. Lett. **91**, 182301, 2003.
 - [5] J. Adams *et al.* (STAR Collaboration), Phys. Rev. Lett. **92**, 052302, 2004.
 - [6] M. Gyulassy and L. McLerran, Nucl. Phys. **A750**, 30 (2005).
 - [7] I. Arsene *et al.* (BRAHMS Collaboration), Nucl. Phys. A **757**, 1, 2005.
 - [8] B. B. Back *et al.* (PHOBOS Collaboration), Nucl. Phys. A **757**, 28, 2005.
 - [9] J. Adams *et al.* (STAR Collaboration), Nucl. Phys. A **757**, 102, 2005.
 - [10] K. Adcox *et al.* (PHENIX Collaboration), Nucl. Phys. A **757**, 184, 2005.
 - [11] C. Adler *et al.* (STAR Collaboration), Phys. Rev. Lett. **87**, 082301, 2001.
 - [12] K. Adcox *et al.* (PHENIX Collaboration), Phys. Rev. Lett. **88**, 192302, 2002.
 - [13] S. S. Adler *et al.* (PHENIX Collaboration), Phys. Rev. Lett. **93**, 152302, 2004.
 - [14] J. Adams *et al.* (STAR Collaboration), Phys. Rev. C **71**, 044906, 2005.
 - [15] W. N. Zhang, M. J. Efaaf, and C. Y. Wong, Phys. Rev. C **70**, 024903 (2004).
 - [16] W. N. Zhang, Y. Y. Ren, and C. Y. Wong, Phys. Rev. C **74**, 024908 (2006).
 - [17] E. Witten, Phys. Rev. D **30**, 272 (1984).
 - [18] S. Pratt, P. J. Siemens, and A. P. Vischer, Phys. Rev. Lett. **68**, 1109 (1992).
 - [19] L. P. Csernai and J. I. Kapusta, Phys. Rev. D **46**, 1379 (1992); Phys. Rev. Lett. **69**, 737 (1992).
 - [20] W. N. Zhang, Y. M. Liu, L. Huo, Y. Z. Jiang, D. Keane, and S. Y. Fung, Phys. Rev. C **51**, 922 (1995).
 - [21] S. Alamoudi *et al.*, Phys. Rev. D **60**, 125003 (1999).
 - [22] J. Randrup, Phys. Lett. **92**, 122301 (2004).
 - [23] C. Y. Wong and W. N. Zhang, Phys. Rev. C **70**, 064904

- (2005).
- [24] W. N. Zhang, S. X. Li, C. Y. Wong, and M. J. Efaaf, Phys. Rev. C **71**, 064908 (2005).
 - [25] W. N. Zhang and C. Y. Wong, talk presented at the XI International Workshop on Correlation and Fluctuation in Multiparticle Production, Nov. 21-24, 2006, Hangzhou, China, arXiv:hep-ph/0702120; C. Y. Wong and W. N. Zhang, talk presented at the XI International Workshop on Correlation and Fluctuation in Multiparticle Production, Nov. 21-24, 2006, Hangzhou, China, hep-ph/0702121.
 - [26] M. Gyulassy, D. H. Rischke, and B. Zhang, Nucl. Phys. **A613**, 397 (1997).
 - [27] H. J. Drescher, F. M. Liu, S. Ostapchenko, T. Pierog, and K. Werner, Phys. Rev. C **65**, 054902 (2002).
 - [28] Y. Hama, T. Kodama, and O. Socolowski Jr, hep-ph/0407264.
 - [29] C. E. Aguiar, T. Kodama, T. Osada, and Y. Hama, J. Phys. G **27**, 75 (2001).
 - [30] G. R. Liu and M. B. Liu, *Smoothed Particle Hydrodynamics: A Meshfree Particle Method*, (in Chinese, translated by X. Han, G. Yang, and H. F. Qiang, Hunan Univisity Press, 2005).
 - [31] M. Gaździcki, M. I. Gorenstein, F. Grassi, Y. Hama, T. Kodama, and O. Socolowski Jr., hep-ph/0309192.
 - [32] R. Andrade, F. Grassi, and Y. Hama, Phys. Rev. Lett. **97**, 202302 (2006).
 - [33] O. Socolowski Jr., F. Grassi, Y. Hama, and T. Kodama, Phys. Rev. Lett. **93**, 182301 (2004).
 - [34] Y. Hama, Rone P.G. Andrade, F. Grassi, O. Socolowski Jr, T. Kodama, B. Tavares, and S. S. Padula, Nucl. Phys. **A774**, 169 (2006).
 - [35] W. L. Qian, R. Andrade, F. Grassi, O. Socolowski Jr., T. Kodama, and Y. Hama, nucl-th/0703078.
 - [36] J. P. Blaizot and J. Y. Ollitrault, Phys. Rev. D **36**, 916 (1987).
 - [37] E. Laermann, Nucl. Phys. A **610**, 1 (1996).
 - [38] D. H. Rischke and M. Gyulassy, Nucl. Phys A **608**, 479 (1996).
 - [39] L. L. Yu, W. N. Zhang, and C. Y. Wong, will be published in Phys. Rev. C.
 - [40] S. Pratt, Phys. Rev. D **33**, 72 (1986); S. Pratt, T. Csörgo, and J. Zimányi, Phys. Rev. C **42**, 2646 (1990).
 - [41] G. Bertsch, M. Gong, and M. Tohyama, Phys. Rev. C **37**, 1896 (1988); G. Bertsch, Nucl. Phys. A **498**, 173c (1989).